Earth Systems and Environment (2022) 6:343–359
https://doi.org/10.1007/s41748-022-00297-y

ORIGINAL ARTICLE

Projected Air Temperature Extremes and Maximum Heat Conditions Over the Middle-East-North Africa (MENA) Region

Athanasios Ntoumos[1] · Panos Hadjinicolaou[1] · George Zittis[1] · Yiannis Proestos[1] · Jos Lelieveld[1,2]

Received: 9 September 2021 / Revised: 13 January 2022 / Accepted: 19 January 2022 / Published online: 28 February 2022

Abstract
This study analyzes projected heat extremes over the Middle-East–North Africa (MENA) region until the end of the twenty-first century with a number of temperature indices based on absolute values and thresholds to describe hot conditions. We use model projected daily near-surface air (2-m) temperature (T_{max} and T_{min}) to derive the indices for the period 1980–2100. The data were taken from 18 CMIP5 models combining historical (1980–2005) and scenario runs (2006–2100 under RCP2.6, RCP4.5, and RCP8.5 pathways). Results show a domain-wide projected warming for all emission scenarios. Our findings for a business-as-usual pathway indicate excessive warming of more than 8 °C in the northern part of the domain (south Europe) for the annual warmest day (TXx) and night (TNx). In the hottest parts of the domain record high temperatures reached 50 °C in the recent past, which could increase to at least 56 °C by the end of the century, while temperatures over 50 °C are expected to occur in a large part of the MENA region. A significant increase is projected in the number of hot days (TX > 40°C) and nights (TN > 30°C) all over the region. For the period of 2071–2100 excessive hot days and nights will become the normal during summer in large parts of the MENA with some locations expected to exceed 180 and 100 days, respectively. Calculations of the corresponding heat index suggest that several areas across the MENA region may reach temperature levels critical for human survival.

Keywords Heat extremes · Emission scenarios · Global climate models · Projections · MENA

1 Introduction

The intensity, frequency, and duration of heatwaves have increased in many regions around the globe since the 1950s (Sillmann et al. 2013a; Perkins-Kirkpatrick and Lewis 2020) and temperatures are expected to further rise in the coming decades owing to climate change (Coumou and Robinson 2013; Sillmann et al. 2013b). Even a modest global mean temperature increase of 2 °C relative to pre-industrial times, could indicate that extreme temperatures in many regions can increase well above 2 °C (Seneviratne et al. 2016). Heat extremes are of high importance to society and ecosystems due to their potentially severe impacts (Allen et al. 2018), for example, they are recognized as the major weather-related cause of premature mortality (Gosling et al. 2009; Mitchell et al. 2016). Over the next few decades, half of the world's population may regularly (every second summer on average) experience regional summer mean temperatures that exceed those of the historically hottest summer (Mueller et al. 2016).

The Middle East-North Africa (MENA) region emerges as a climate change hotspot with strong temperature increases and rainfall reductions since the middle of the twentieth century (Lelieveld et al. 2012; Tanarhte et al. 2012; Zittis 2018; Ntoumos et al. 2020). This region has been historically exposed to high temperatures and dryness. For example, on July 21, 2016, a temperature of 53.9 °C was recorded in Mitribah, Kuwait, the third highest WMO-recognized temperature extreme (Merlone et al. 2019). Studies suggest that climate warming in the MENA follows a differential seasonal response with much stronger warming in summer than in winter (Sillmann et al. 2013b; Lelieveld et al. 2016). Climate projections indicate that in MENA, heat extremes intensification is very likely to continue throughout the twenty-first century (Zittis et al. 2016; El-Samra et al.

✉ Athanasios Ntoumos
a.ntoumos@cyi.ac.cy

[1] Climate and Atmosphere Research Centre (CARE-C), The Cyprus Institute, 2121, Nicosia, Cyprus

[2] Department of Atmospheric Chemistry, Max Plank Institute for Chemistry, 55020 Mainz, Germany

Table 1 Set of 18 CMIP5 global models with their respective horizontal resolution, equilibrium climate sensitivity (ECS) and transient climate response (TCR) for CO_2 doubling

Model	lon (°)	lat (°)	ECS (°C)	TCR (°C)	References
BCC-CSM1.1	2.81	2.79	2.8	1.7	Tongwen et al. (2014)
BNU-ESM	2.81	2.79	4.1	2.6	Ji et al. (2014)
CanESM2	2.81	2.79	3.7	2.4	Chylek et al. (2011)
CCSM4	1.25	0.94	2.9	1.8	Gent et al. (2011)
CNRM-CM5	1.40	1.40	3.3	2.1	Voldoire et al. (2013)
CSIRO_Mk3.6.0	1.87	1.87	4.1	1.8	Collier et al. (2011)
GFDL-CM3	2.50	2.00	4.0	2.0	Griffies et al. (2011)
GFDL-ESM2G	2.50	2.00	2.4	1.1	Dunne et al. (2012)
GFDL-ESM2M	2.50	2.00	2.4	1.3	Dunne et al. (2012)
HadGEM2-AO	1.87	1.25	4.6	2.4	Collins et al. (2008)
HadGEM2-ES	1.87	1.25	4.6	2.5	Collins et al. (2008)
IPSL-CM5A-LR	3.75	1.89	4.1	2.0	Dufresne et al. (2013)
IPSL_CM5A-MR	2.50	1.26	4.1	2.0	Dufresne et al. (2013)
MIROC5	1.40	1.40	2.7	1.5	Watanabe et al. (2010)
MIROC-ESM	2.81	2.79	4.7	2.2	Watanabe et al. (2011)
MIROC-ESM-CHEM	2.81	2.79	4.6	2.2	Watanabe et al. (2011)
MPI-ESM-LR	1.87	1.87	3.6	2.0	Giorgetta et al. (2013)
MRI-CGCM3	1.12	1.12	2.6	1.6	Yukimoto et al. (2012)

2018; Legasa et al. 2020; Ozturk et al. 2021). According to the business-as-usual pathway, by the end of the twenty-first century about half of the MENA population (approximately 600 million) will be exposed to excessively high temperatures (up to 56 °C) while extreme heat conditions will likely last for several weeks (Zittis et al. 2021). If the projected high temperatures become reality, they will exceed the threshold for human adaptability and parts of the region may become inhabitable for humans (Pal and Eltahir 2016; Almazroui 2020).

Analysis of projections from the Coupled Model Intercomparison Project Phase 5 (CMIP5) (Taylor et al. 2012) can provide estimates for future changes in temperature related extremes, which vary according to world region, emissions scenario, and time period in the twenty-first century. From the work of Sillmann et al. (2013b), it emerges that the projected changes in extreme indices of temperature will be more pronounced in and around the Mediterranean region compared to other areas of the world, indicating a considerable intensification of heat stress. Lelieveld et al. (2016) used CMIP5 global model projections and derived for a high emissions scenario (RCP8.5), that (averaged over the MENA) the warmest nights will surpass 30° by the middle of the century and increase further to above 34 °C by the end of the century. The maximum daytime temperature during the hottest days may increase to nearly 47 °C by the middle of the century, and reach nearly 50 °C by the end of the century in the RCP8.5 scenario.

Considering the challenges arising from the intensification of heat extremes, it is important to acquire a more detailed picture of the projected changes over the MENA region. In a recent study, Ntoumos et al. (2020) compared ETCCDI indices computed from observations and CMIP5 model simulations, and found that the GCMs were generally able to reproduce the historical trend patterns of the temperature-related extreme indices. It was also shown that CMIP5 models exhibit domain-wide strong and statistically significant warming over the last decades. Here, we extend this analysis until the end of twenty-first century, by revealing certain aspects of future temperature extremes under different emission scenarios and GCM climate sensitivity. Particular emphasis is given yo the projected highest (maximum) temperatures and heat stress, approaching the limit of human health tolerance, as well as the sub-regional hotspots where these occur.

Specifically, following the description of the pertinent climate data and the definitions of temperature extremes (Sect. 2), we document their changes in space and time according to different RCP scenarios (Sect. 3) and reveal the magnitude and duration of the projected maximal temperatures for the scenario with high greenhouse gas (GHG) concentrations (Sect. 4) (Table 1).

2 Data and Methodology

2.1 Global Climate Models and Scenarios

We consider the output of 18 CMIP5 models from the historical forcing runs until 2005, and beyond this year from the Representative Concentration Pathway (RCP) model projections (Vuuren et al. 2011) for radiative forcing values

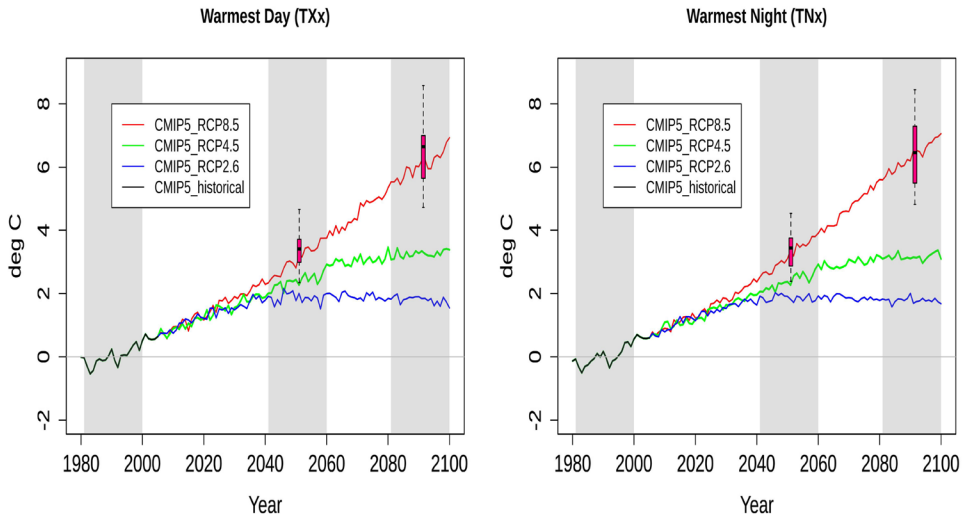

Fig. 1 MENA averages of absolute temperature indices over land as simulated by the CMIP5 ensemble for the RCP2.6 (blue), RCP4.5 (green), and RCP8.5 (red) displayed as anomalies from the reference period 1981–2000. The box-and-whisker plots show the interquartile ensemble spread (box) and outliers (whiskers) for 18 CMIP5 model simulations of the RCP8.5 scenario over the respective future time periods (2041–2060 and 2081–2100) as indicated by the shading

2.6, 4.5 and 8.5 W/m^2. Daily maximum and minimum near-surface air temperatures were retrieved from the Earth System Grid Federation (ESGF) data portal[1]. Model selection was done based on data availability for the different RCP scenarios. Here, we consider only one (typically the first) ensemble member of each model. The data were acquired from the historical simulations for the period 1980–2005 and scenario projections for the period 2006–2100 (under the RCP2.6, RCP4.5 and RCP8.5). The complete set is summarized in Table 2.

2.2 Extreme Heat Indices

To detect changes in climate extremes, we used indices based on daily maximum and daily minimum near surface temperatures (TX and TN), facilitated by a standard procedure that defines a set of temperature based indices, a subset of the Expert Team on Climate Change Detection and Indices (ETCCDI) (Karl et al. 1996). These indices are also defined and described in detail by Tank et al. (2009) and Zhang et al. (2011). From the longer list of these indices, we focus on the following four, which are related to extreme heat and from the way they are defined, are pertinent to the warm part of the year and the peak temperatures during summer. The used indices are split into two categories as described below.

Absolute Indices These are the Warmest Day and Warmest Night, defined as the maximum of TX (labelled TXx) and the maximum of TN (labelled TNx), respectively, in a year.

Threshold Indices Because of the very high summertime temperatures prevailing in MENA region, we define as Hot Days the number of days per year with TX > 40 °C and Hot Nights the number of days per year with TN > 30 °C.

2.2.1 Heat Index

We also examine the Heat Index (HI) to account for the heat stress induced by the combined effects of high temperature and high humidity. HI is interpreted as what the temperature feels like to the human body when relative humidity is combined with the air temperature and is defined by the U.S. National Oceanic and Atmospheric Administration (NOAA) and is used for issuing heat warnings. HI is calculated as multiple linear regression with temperature and relative humidity as input variables (Rothfus 1990; Steadman 1979). For our calculations we used daily mean temperature (TG) and relative humidity (RH) from the CMIP5 output.

2.3 Data Processing and Calculations

The data analysis is restricted to a geographical domain representative of the MENA region that extends from 12° N to 46° N, and from 20° W to 64° E, covering North Africa, Middle East, and the Mediterranean (including parts of south Europe). For the purpose of comparing indices among datasets of different native spatial resolution, we regridded the original daily temperature data to a common 45 × 19 grid (1.87° × 1.87°) for MENA. For the CMIP5 data, the indices were derived from the T_{max} and T_{min} daily timeseries for each model and RCP scenario, and the multi-model averages were subsequently calculated.

Regarding the significance of the projected changes in heat extremes, we follow the definition used in the IPCC's Atlas of Global and Regional Climate Projections (IPCC 2013b). More specifically, a change is considered significant when its signal is larger than the interannual variability

[1] https://esgf-node.llnl.gov/projects/esgf-llnl/

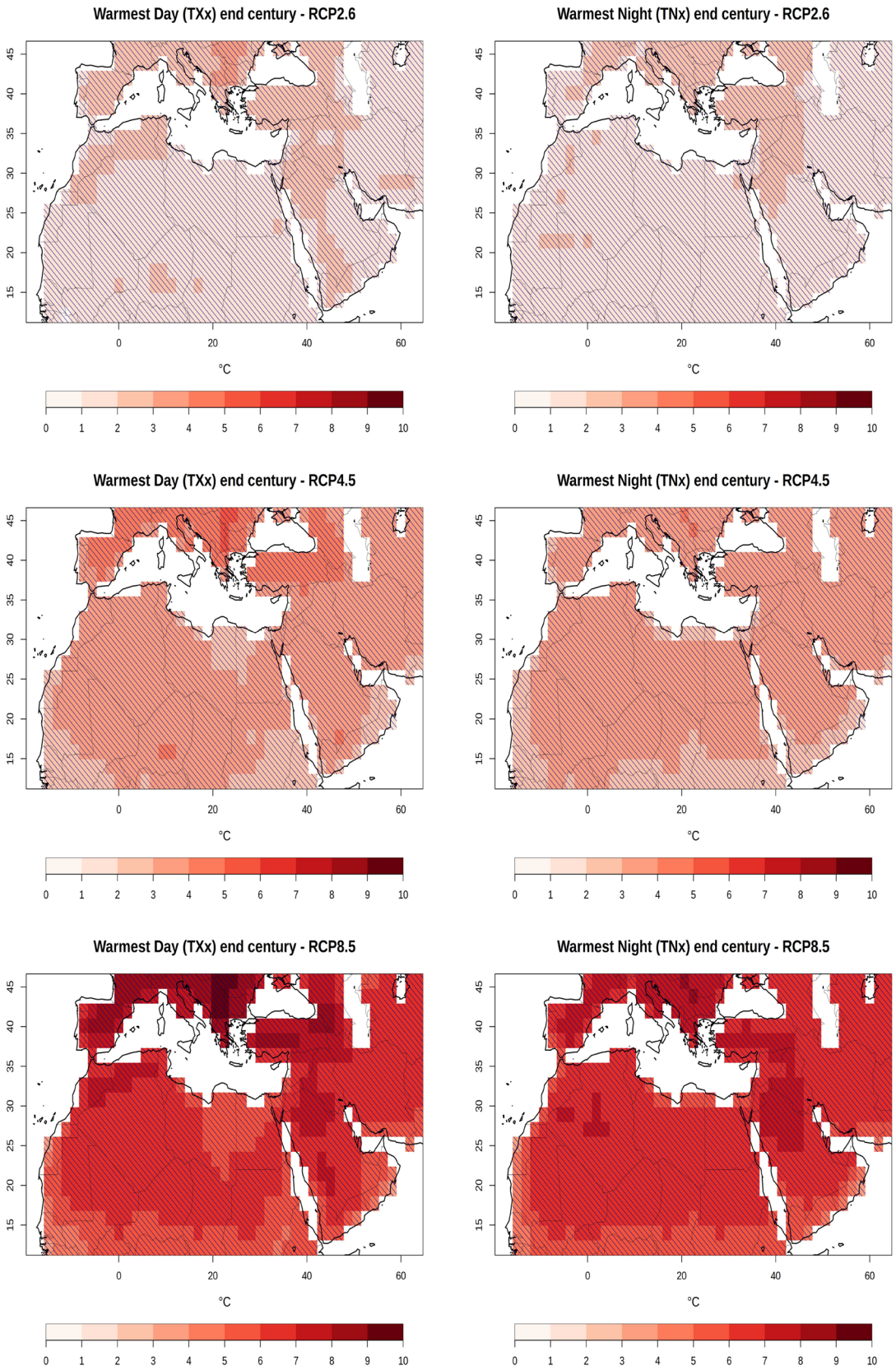
Warmest Day (TXx) end century - RCP2.6
Warmest Night (TNx) end century - RCP2.6
Warmest Day (TXx) end century - RCP4.5
Warmest Night (TNx) end century - RCP4.5
Warmest Day (TXx) end century - RCP8.5
Warmest Night (TNx) end century - RCP8.5
°C

◂**Fig. 2** The multimodel mean of temporally averaged changes in the Warmest Day (TXx, left) and the Warmest Night (TNx, right) over the time period 2081–2100 displayed as differences (in °C) relative to the reference period (1981–2000) for RCP2.6 (top), RCP4.5 (middle), and RCP8.5 (bottom). The hatching represents significant changes

of the reference historical period. We derive the interannual variability directly from the calculation of the standard deviation for temperature.

A simple bias adjustment method was implemented to remove any systematic errors in the model output to enhance the confidence in the projected absolute values of the temperature extremes. For this purpose, the WFDE5 bias-adjusted ERA5 reanalysis was used (Cucchi et al. 2020). The WFDE5 dataset has been generated using the WATCH Forcing Data (WFD) methodology applied to surface meteorological variables from the ERA5 reanalysis and is provided at 0.5 spatial resolution. Here the projected heat extremes were corrected based on their climatological biases from the WFDE5. More specifically, the multimodel mean biases from the WFDE5 were calculated for the reference period. Subsequently, the projected model indices for the future period were adjusted by subtracting the reference period biases (as detailed in Sect. 4). Since the heat index is not available in the WFDE5 output we used the Global Land Data Assimilation System (GLDAS) dataset (Mistry 2020). GLDAS is a high-spatial resolution (0.25 °), global-gridded database of multiple human discomfort indices.

3 Changes in Heat Extremes

In this part of the study, we analyze the projected changes in heat extremes in space and time according to the different RCP scenarios.

3.1 Absolute Indices

3.1.1 Temporal Evolution

We begin our analysis with the temporal evolution of the absolute indices averaged for the MENA domain (land only). Figure 1 depicts the temporal evolution of the warmest day and warmest night displayed as anomalies from the reference period 1981–2000. Here, we plot CMIP5 data for the historical (1980–2005) and from 2006 to 2100, separately, for the three scenario runs (2006–2100 under RCP2.6, RCP4.5, and RCP8.5). In accordance with the global average temperature projections (Knutti and Sedláček 2013), differential warming due to the RCP scenarios is discernible only after 2030.

For all scenarios, both TXx and TNx are projected to increase until the end of the twenty-first century. The multimodel median increase in TXx and TNx during 2081–2100 is 6.1 °C and 6.3 °C, respectively, in RCP8.5. The warming is less pronounced for the other two RCP scenarios: for TXx and TNx the projected median increase is 1.8 °C for both in RCP2.6, and 3.3 °C and 3.2 °C, respectively, in RCP4.5.

In addition, the ensemble model spread for RCP8.5, indicated with the box-plots, is similar for both indices. A correlation analysis (not shown) between the models' equilibrium climate sensitivity (ECS) and the derived MENA-average changes, reveals that models with higher ECS tend to show a more pronounced warming. For both indices of temperature extremes we find, for RCP8.5, a strong correlation ($r = 0.8$, Figure S1).

3.1.2 Spatial Patterns

We present the spatial changes of temperature indices of extremes as simulated in the CMIP5 ensemble for all three RCP's for the time period 2081–2100. Figure 2 depicts the

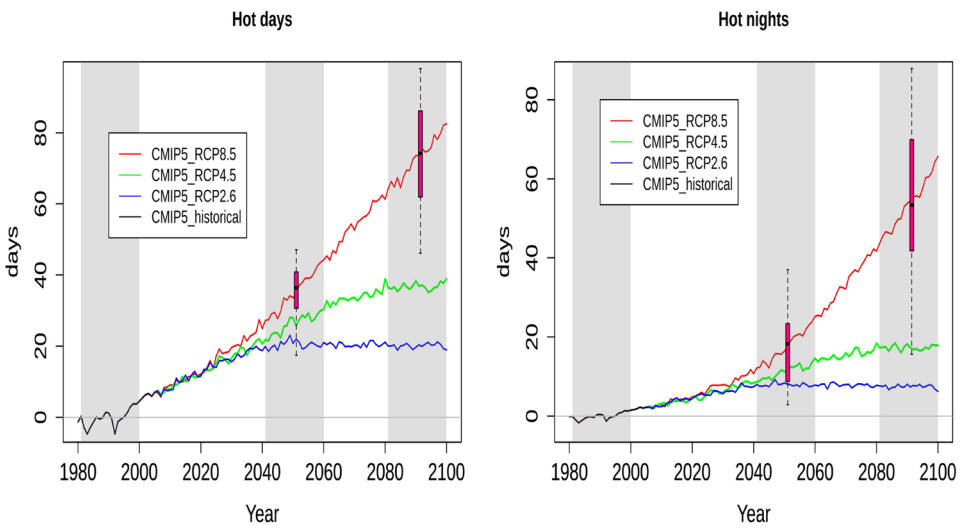

Fig. 3 MENA averages of threshold temperature indices over land as simulated by the CMIP5 ensemble for the RCP2.6 (blue), RCP4.5 (green), and RCP8.5 (red) displayed as anomalies from the reference period 1981–2000. The box-and-whisker plots show the interquartile ensemble spread (box) and outliers (whiskers) for 18 CMIP5 model simulations of the RCP8.5 scenario over the respective future time periods (2041–2060 and 2081–2100) as indicated by shading

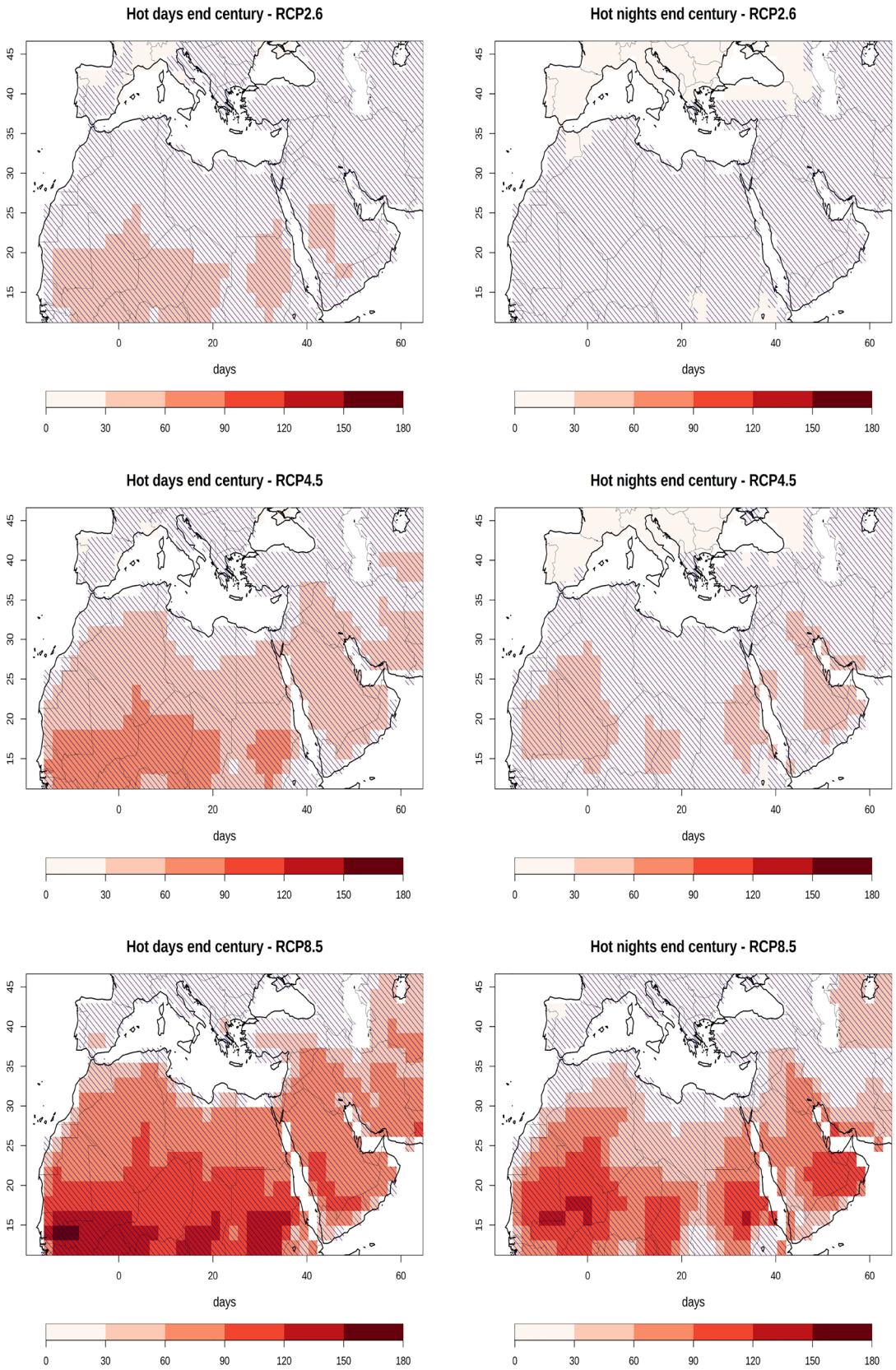
Hot days end century - RCP2.6
Hot nights end century - RCP2.6
Hot days end century - RCP4.5
Hot nights end century - RCP4.5
Hot days end century - RCP8.5
Hot nights end century - RCP8.5
days
0 30 60 90 120 150 180

◂**Fig. 4** The multimodel mean of temporally averaged changes in the annual number of hot days (TX > 40 °C, left) and hot nights (TN > 30 °C, right) over the time period 2081–2100 displayed as differences (in °C) relative to the reference period (1981–2000) for RCP2.6 (top), RCP4.5 (middle), and RCP8.5 (bottom). The hatching represents significant changes

changes relative to the 1981–2000 reference period for the warmest day and night (TXx and TNx, respectively).

The results generally indicate an intensification of heat extremes with increasing radiative forcing of the warming patterns, which have already been observed in the region, in model simulations of the historical and present climate (Ntoumos et al. 2020). These warming patterns are quite similar for both indices. The changes are significant over the entire MENA, for all emission scenarios. Both TXx and TNx exhibit stronger increases in the northern part of the MENA domain (South Europe) which is in line

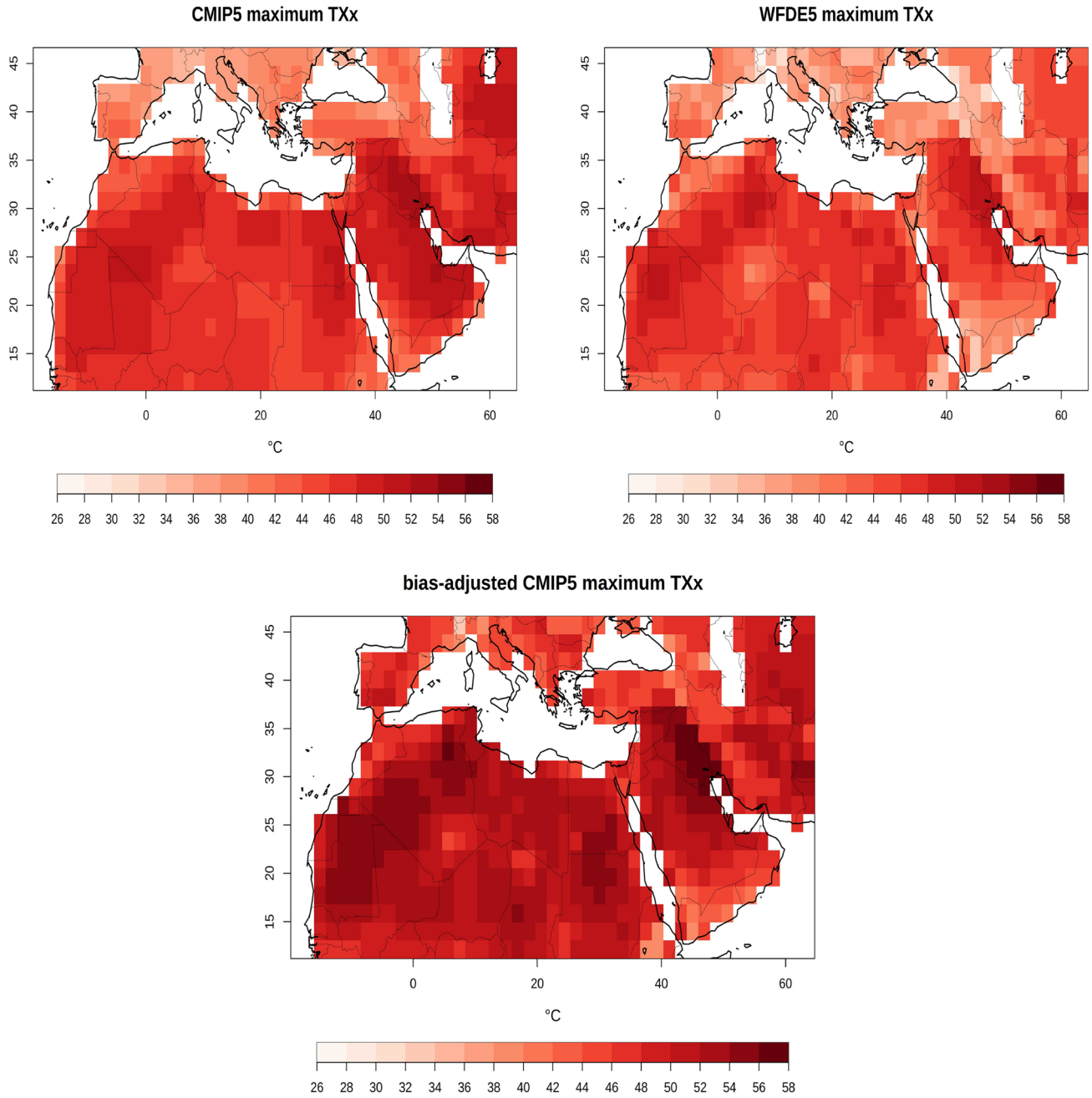

Fig. 5 Spatial representation of the maximum TXx for the multimodel ensemble mean (top, left), WFDE5 reanalysis (top, right) for the period 1990–2019, and multimodel ensemble mean(bias adjusted) for the 2071–2100 (bottom)

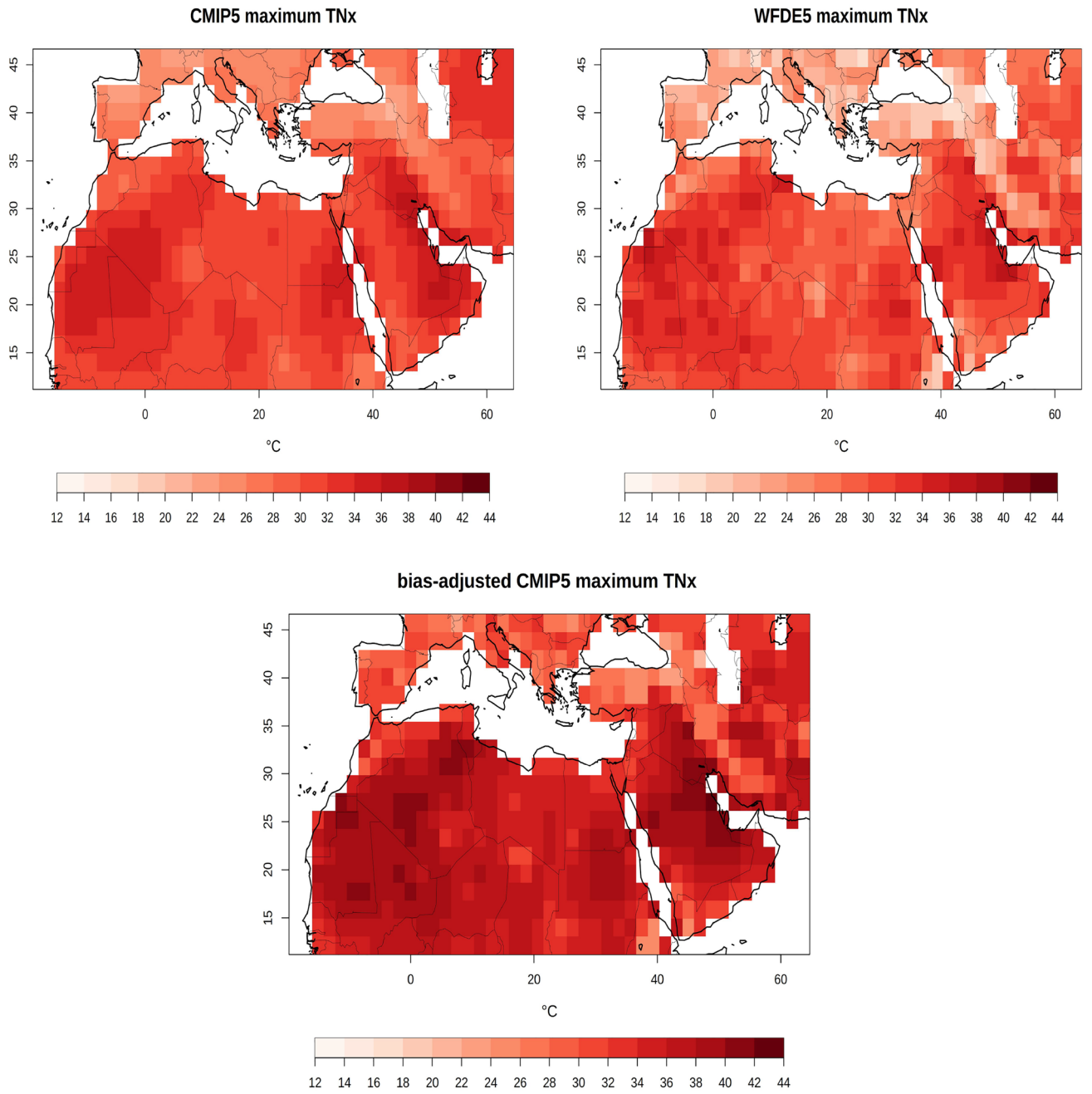

Fig. 6 Same as Fig. 5 but for the maximum TNx

with relevant global (Sillmann et al. 2013b) and regional (Lelieveld et al. 2016) studies. These results are also in agreement with recent CMIP6 based studies (Vogel et al. 2020; Almazroui et al. 2021), in which similar patterns of warming have been reported. According to Almazroui et al. (2021), the CMIP6 multimodel ensemble indicates a substantial increase in TXx over the Mediterranean region and adjacent parts of Europe, in contrast with areas near the tropics. The stronger warming at the northern part of the MENA domain can be linked to soil moisture feedbacks (Russo et al. 2019) and precipitation deficits (Mueller and Seneviratne 2012), which can amplify heat conditions. On the other hand, this positive soil moisture - air temperature feedback is absent in the arid areas of MENA, since rainfall and soil moisture in summer are practically zero (Zittis et al. 2014). According to RCP8.5, TXx is projected to increase up to 10 °C over the Balkan region, while a 1–2 °C less intense warming is projected for the TNx index. A similar pattern of regional changes in TXx and TNx is seen for RCP4.5 and RCP2.6, albeit

less pronounced as compared to RCP8.5. A quantitative overview of the mean indices changes in different parts of the MENA is shown in Table S1.

3.2 Threshold Indices

3.2.1 Temporal Evolution

Figure 3 shows the temporal evolution of the median changes in the number of hot days (TX > 40 °C) and hot nights (TN > 30 °C) per year relative to 1981–2000 reference period averaged for the MENA domain. The number of hot days increases by about 20 days at the end of twenty-first century in RCP2.6. For RCP4.5 the median increase in the number hot days/year is 37 and reaches 73 for RCP8.5. The multimodel median increase in the number of hot nights/year is 54 for RCP8.5 while is less pronounced for RCP4.5 and RCP2.6, about 17 and 7 nights, respectively.

The spread for these two indices is illustrated by the box-and-whisker plots, showing that the number of hot nights can increase to more than 60 days per year. This can be related to differences among models in simulating processes that control nighttime temperatures such as regional circulation changes, cloud cover, and soil moisture (Morak et al. 2011). It is also worth noting that for the number of hot days we find a significant correlation ($r = 0.84$) between the models' ECS and the average projected changes over MENA, while for the number of hot nights no correlation is found (Figure S1).

3.2.2 Spatial Patterns

In Fig. 4, we show the changes relative to the 1981–2000 reference period of the hot days and nights (days with TX > 40 °C and TN > 30 °C, respectively) per year. The spatial patterns and magnitude of the projected changes are quite similar for the two indices. The strongest warming is observed in the southern parts of the MENA which is expected from the prevailing lack of soil moisture in those areas so that the temperatures adjust to sensible heat only, without any contribution by latent heating. For the more temperate Mediterranean, where the soils are not notoriously dry, this increase is weaker (0–30 days), especially compared to other areas around MENA. Only for the RCP8.5 scenario the increase in the number of hot days is more than 30, over parts of the Iberian Peninsula and the Balkans (see Table S1).

The greatest changes in the number of hot days, exceeding 90 (3 months) and reaching 150 (5 months), are simulated for RCP8.5 in sub-regions near the tropics with relatively high temperatures throughout the year. Smaller increases are observed for the other two scenarios with the respective changes below 90 and 60 days, for RCP4.5 and RCP2.6, respectively. In addition, the change in the number of hot nights surpasses 90 in parts of North Africa and the Arabian peninsula for RCP8.5.

4 Projected Maximum Temperatures

In this part of the study, we extend the analysis of heat extremes to the highest projected temperatures over the MENA as well as the absolute numbers of hot days and nights per year, focusing on the RCP8.5 scenario results. We also add to our analysis the Heat Index to account for humidity and indicators that are related to heat stress impacts. We now use the 1990–2019 as reference period to include an up-to-date account of the current heat extremes. An overview of the future extremes in different parts of MENA can be found in Table 2.

4.1 Absolute Indices

4.1.1 Maximum of TXx

Figure 5 illustrates the maximum values of TXx obtained from the ensemble of the 18 CMIP5 models and the WFDE5 reanalysis. The maps reveal the highest daily temperatures over each period indicated, for every grid point of the MENA analyzed. On the top we show the maximum of TXx over the 1990–2019 period for the CMIP5 ensemble mean (using the model output of the historical run up to 2005 and of the RCP8.5 thereafter) and the WFDE5 reanalysis. The bottom map refers to the 2071–2100 period as projected by the CMIP5 ensemble for RCP8.5 with the values adjusted based on the CMIP5 model biases from WFDE5 of 1990–2019 climatology.

For the control period (1990–2019) the spatial distribution and magnitude of the CMIP5 derived index are in good agreement with the ones obtained by WFDE5. The CMIP5 ensemble mean captures nicely the observed hottest areas within the region (parts of northern Africa and the Middle East with the highest occurring temperatures approaching and even surpassing 50 °C). In the northern parts of the domain, where milder conditions exist, the CMIP5 ensemble tends to overestimate the index, especially over high terrain areas. This slight warm bias can be attributed to the coarse spatial resolution of the global models compared with the WFDE5, which more accurately represents altitude differences. The effect of bias-adjustment to the CMIP5 data is also illustrated in Figure S2.

Regarding the projections for the end of the century period (2071–2100) the "hotspot" areas remain the same

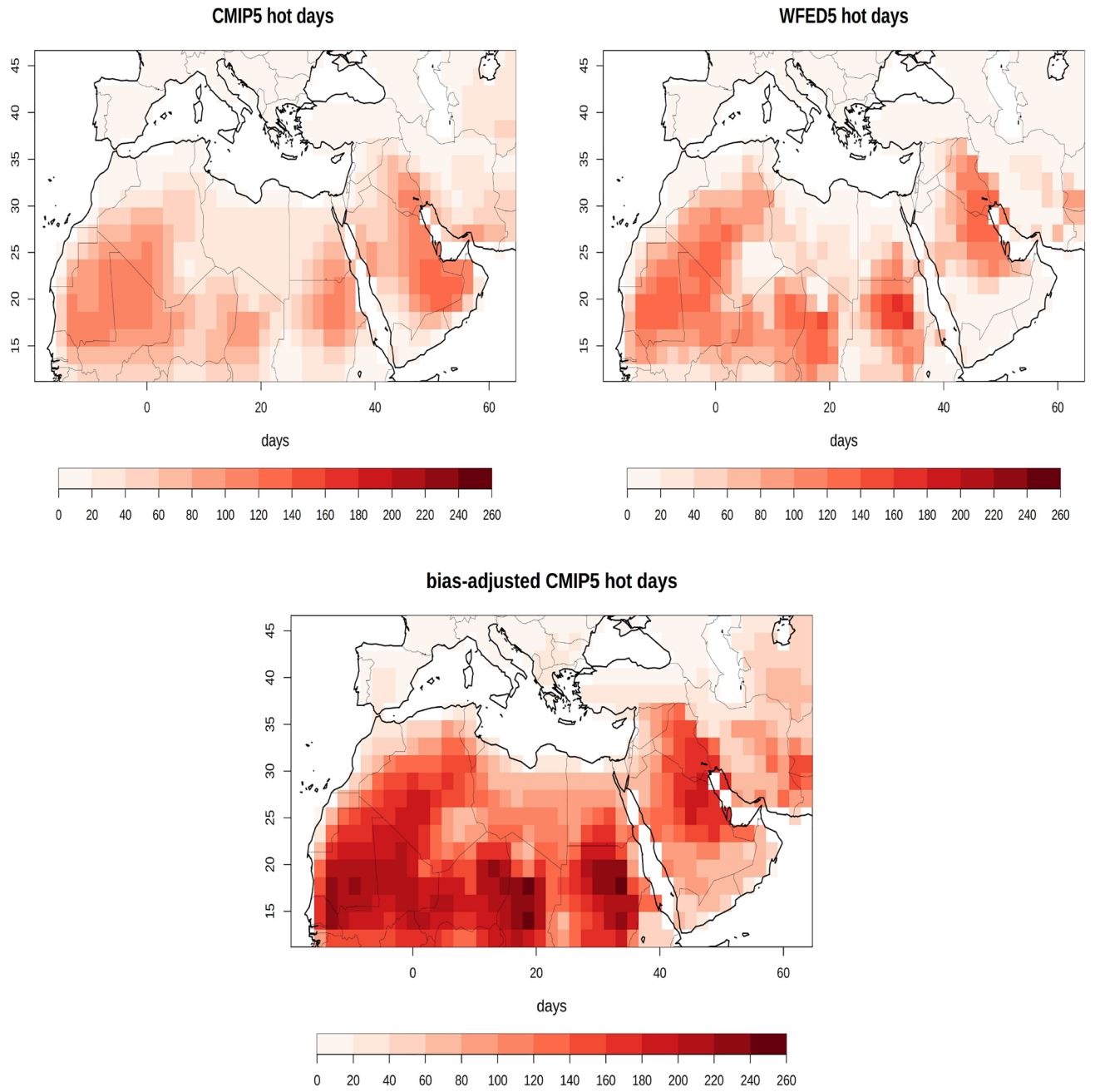

Fig. 7 Same as Fig. 5 but for the hot days

(parts of northern Africa, Gulf region/Iraq). A large part of the MENA region is projected to experience daily temperatures over 50 °C by the end of the century. Especially over the northern part of the Gulf and Iraq, CMIP5 ensemble projects temperatures over 56 °C, higher than the currently occurring worldwide heat records (Matthews 2020). It is worth noting that quite a few ensemble members (not shown) indicate future record high temperatures reaching and even surpassing 60 °C.

4.1.2 Maximum of TNx

The maximum values of the TNx index (record high nighttime temperatures) from the CMIP5 ensemble and the WFDE5 reanalysis are presented in Fig. 6. The same method of bias adjustment was followed.

The CMIP5 models capture quite well the observed "hotspot" areas of the index (with maximum of TNx over 30 °C) over the Gulf region, parts of northwest Africa and some areas around the Red Sea. Model warm bias exist

over the northern part of the domain, especially in mountainous regions due to the coarse model resolution. For the 2071–2100 period most areas in north Africa and the Middle-East exhibit daily minimum temperatures over 35 °C. Parts of northwest Africa and mainly coastal areas of the Gulf will record nighttime temperatures over 40 °C at the end of the century.

4.2 Threshold Indices

We next extend the previous analysis of single-day extreme heat events to the threshold indices of the number of days with TX >40 °C and TN > 30 °C.

4.2.1 Hot Days

Figure 7 depicts the average annual number of hot days (TX > 40 °C) from the CMIP5 ensemble and the WFDE5 reanalysis for the control period 1990–2019 and for the future period 2071–2100. The future values (bottom map) have been adjusted using the model biases from the WFDE5 in the control period.

In general, CMIP5 models capture very well the hotspot areas within MENA. One noticeable exception is the southern part of the Arabian peninsula where the CMIP5 models simulate a considerable number of hot days (> 50) whereas WFDE5 presents lower values (< 20). For the present period (1990–2019) the number of hot days around the Mediterranean is close to zero whereas in parts of North Africa and the Gulf reaches 100-120 days per year.

For the future period (2071–2100) the bias adjusted CMIP5 ensemble projects that the annual number of hot days will reach and surpass 180 days in regions near the tropics and the Gulf. In other words, these areas may record temperatures over 40 °C on a daily basis for more than the half of the year. Lower, but still significant values are projected in the northern part of MENA. For instance, the number of hot days in southern Balkans will be 20–40 days.

4.2.2 Hot Nights

In a similar way, the number of hot nights (TN > 30 °C) is presented in Fig. 8 for CMIP5 models and WFDE5 reanalysis.

For the present period (1990–2019), the occurrence of minimum temperatures over 30 °C is limited to three MENA sub-regions and it is more pronounced (in magnitude and spatial extent) in the CMPI5 data. According to the CMIP5 ensemble, areas around the Gulf, the Red Sea and north-west Africa reach a number of 30 hot nights per year. The occurrence of hot nights is even more limited in WFDE5 with only coastal regions around the Gulf exhibiting a similar amount of hot nights.

While in the present period hot nights are a rare event for most of the MENA region, they will become more common (in frequency and spatial occurrence) at the end of the century. For the 2071–2100 period, the CMIP5 ensemble projects that the hottest areas will surpass 90 days (3 months) of hot nights per year. Even the cooler areas at the north of MENA domain could record 10–30 days with minimum temperatures over 30 °C.

4.3 Heat Index

Figure 9 shows the average annual maximum Heat Index (HIx) from the CMIP5 ensemble and the GLDAS dataset for the control period 1990–2018 and for the future period 2071–2100. Here, we exclude the year 2019 due to the unavailability of GLDAS data for the year 2018. Similar to the other indices, a bias adjustment was applied based on the model biases from the GLDAS dataset in the control period.

For the control period (1990–2018), we find that the CMIP5 ensemble mean captures the areas with the highest HIx. These areas are the broader area of the Gulf, large part of west Africa and some areas around the Red sea with HIx over 40 °C. The models show warm biases relative to the GLDAS dataset, due to their limited ability to realistically simulate humidity.

At the end of the century (2071–2100), the bias-adjusted ensemble projects a strong increase in the HIx. The MENA-average warming before bias adjustment is 11 °C compared to 1990–2018 (see also Figure S5). On the other hand, both TXx and TNx indices show a rather moderate increase of about 5 °C over the same period. This is in line with global studies (Russo et al. 2017; Schwingshackl et al. 2021) in which the Heat Index is projected to increase sharply in all regions of the globe even for a moderate increase in mean temperature and temperature related indices, pointing to the future amplification of heat stress. Bias-adjusted HIx is projected to approach and in some areas surpass the 54 °C threshold in areas around the Gulf, the Red Sea and in Sub-Saharan Africa where high temperature and relatively high humidity values are combined. The Heat Index values above the 54 °C are classified as "extreme danger" according to the NOAA heat warning scale[2]. Note that the Heat Index might be underestimated because it is calculated using daily mean values of relative humidity and temperature instead of relative humidity occurring at the time of the daily maximum temperature.

[2] https://www.wrh.noaa.gov/psr/general/safety/heat

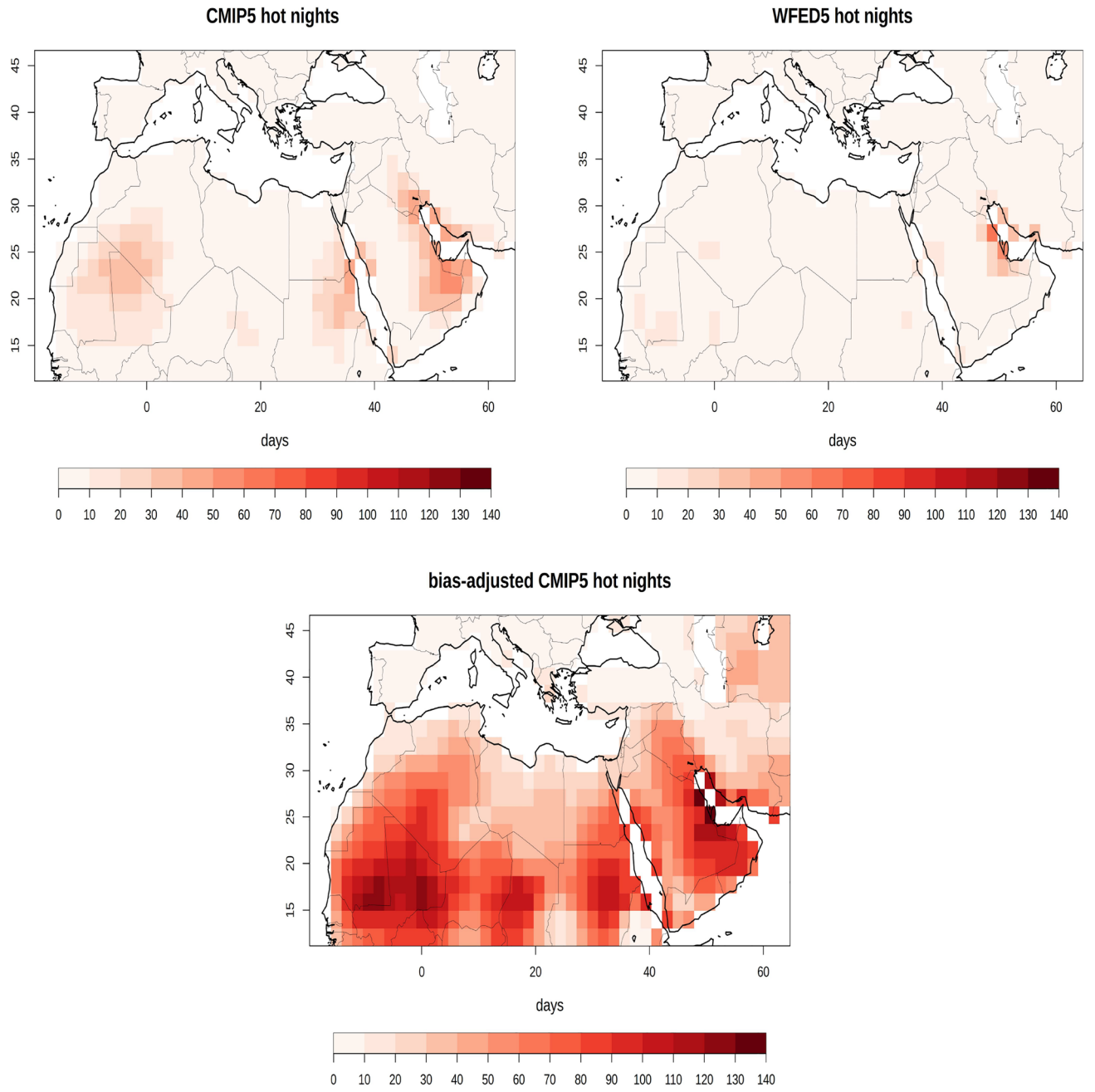

Fig. 8 Same as Fig. 5 but for the hot nights

Table 2 Multi-model bias-adjusted values over the time period 2071–2100

Domain	Max TXx (°C)	Max TNx (°C)	Hot days	Hot nights	HIx(°C)
MENA	50.1 ± 1.4	35.0 ± 1.1	104 ± 12	49 ± 17	45.4 ± 2.6
Mediterranean	47.2 ± 1.6	31.3 ± 1.3	29 ± 16	12 ± 12	39.6 ± 1.7
Sahara	52.3 ± 1.2	36.8 ± 1.3	130 ± 14	53 ± 21	45.8 ± 3.4
Middle-East	51.5 ± 1.5	37.2 ± 1.1	116 ± 12	66 ± 19	47.0 ± 3.0

Values are displayed for different indices over different subdomains within MENA. The subdomains are displayed in Figure S5. The ± ranges indicate 1σ standard deviations of the mean

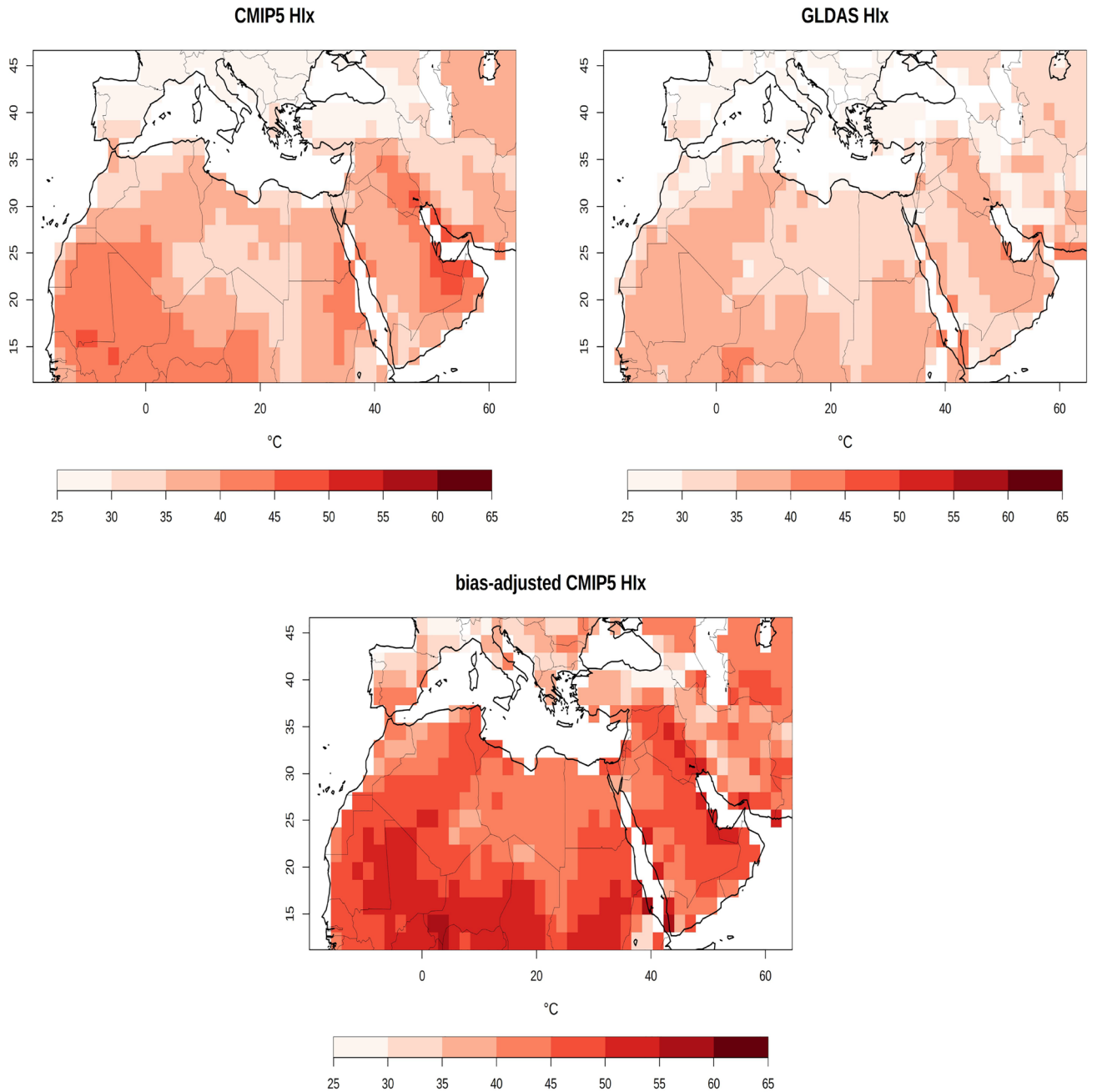

Fig. 9 Spatial representation of the mean annual maximum of Heat Index (HIx) of the multimodel ensemble mean (top, left), GLDAS dataset (top, right) for the period 1990–2018, and multimodel ensemble mean(bias adjusted) for the 2071–2100 (bottom)

5 Summary and Conclusions

This study analysed the temporal evolution and spatial patterns in the magnitude and frequency of temperature extremes, with emphasis on the excessively hot conditions projected for the end of the twenty-first century. For this, we used the output from 18 CMIP5 models from historical runs (1980–2005) and emission scenario simulations (2006–2100 under RCP2.6, RCP4.5, and RCP8.5). To evaluate changing heat extremes we included a subset of absolute and threshold indices defined by the ETCCDI. The definition of the threshold indices (i.e summer days and tropical nights) was modified to be more relevant with the hot summer temperatures that prevail in the MENA.

Spatial patterns of change in the indices were analyzed for the period of 2081–2100 compared to the reference period of 1981–2000. Findings suggest a domain-wide warming for all the emission scenarios. For the warmest day (TXx) and

the warmest night (TNx) models show a consistent pattern with stronger warming in the northern part of the MENA, exceeding 8 °C in RCP8.5. The opposite pattern is found for the number of hot days (TX > 40 °C) and hot nights (TN > 30 °C), which is expected due to the warmer background climate of the southern areas. In the hottest areas of the region the models project changes that exceed 120 and 90 days for hot days and nights, respectively, progressively increasing throughout the century responding to the increasing radiative forcing.

The highest obtained temperatures were also derived from the maximum of TXx and TNx according to the RCP8.5 scenario. The accuracy of these projected values was improved by implementing a bias adjustment method based on the model spatial differences from the WFDE5 reanalysis. For the 2071–2100 period, a large part of the MENA region could exceed 50 °C during the strongest heat events and may even surpass 56 °C in parts of Gulf and Iraq. For the maximum of TNx, the CMIP5 ensemble shows a widespread occurrence of nights with minimum temperatures over 35 °C and over 40 °C in the coastal areas around the Gulf.

The number of hot days (TX > 40 °C) is close to zero in the more temperate areas of the Mediterranean for the present period (1990–2019), while it approaches 100 days in the hottest parts of the region. At the end of the twenty-first century (2071–2100) days with maxima over 40 °C seems to become the ”new normal” occurring in more than half of the days in a year (180 days) in many locations within MENA. The occurrence of hot nights (TN > 30 °C) is limited in the present period (1990–2019) for most of MENA. This is projected to change dramatically until the end of the century with a large part of MENA recording nighttime temperatures above 30 °C for the entire summer season. Especially, parts of Gulf will exceed 4 months (120 days) of hot nights.

The effect of relative humidity on heat extremes was also considered, in the calculation of the Heat Index. It is shown that HIx increases sharper relative to the TXx index, highlighting the amplifying effect of humidity on the combined heat. Projected HIx index values in several areas across MENA region are projected to reach levels critical for human survival.

In the already environmentally stressed MENA, a strong increase in hot weather extremes is anticipated. According to the business-as-usual scenario, areas in MENA may have to deal with extremely high temperatures that will exceed the currently occurring worldwide records (Matthews 2020). This will aggravate the impacts of heat extremes on human health, as limits to human comfort and survivability are being reached. Moreover, extreme heat is expected to impact various sectors like agriculture, energy supply, that will challenge social and political systems in the region (Waha et al. 2017). It is thus imperative the planning for adaptation measures that will ameliorate the adverse impacts of extreme heat, especially in the most strongly affected areas of the region revealed in this study.

Supplementary Information The online version contains supplementary material available at https://doi.org/10.1007/s41748-022-00297-y.

Acknowledgements This work was co-funded by the European Regional Development Fund and the Republic of Cyprus through the Research Innovation Foundation CELSIUS Project EXCELLENCE/1216/0039. It was also supported by the EMME-CARE project that has received funding from the European Union's Horizon 2020 Research and Innovation Programme, under grant agreement no. 856612, as well as matching co-funding by the Government of the Republic of Cyprus.

Declarations

Conflict of interest The authors declare that they have no conflict of interest.

References

Allen M, Dube O, Solecki W, Aragón-Durand F, Cramer W, Humphreys S, Kainuma M, Kala J, Mahowald N, Mulugetta Y, Perez R, Wairiu M, Zickfeld K (2018) Chapter 1: framing and context. In: Global Warming of 1.5°C. An IPCC special report on the impacts of global warming of 1.5°C above pre-industrial levels and related global greenhouse gas emission pathways, in the context of strengthening the global response to the threat of climate change, sustainable development, and efforts to eradicate poverty

Almazroui M (2020) Summer maximum temperature over the gulf cooperation council states in the twenty-first century: multimodel simulations overview. Arab J Geosci. 10.1007/s12517-020-05537-x/Published, 10.1007/s12517-020-05537-x

Almazroui M, Saeed F, Saeed S, Ismail M, Ehsan MA, Islam MN, Abid MA, O'Brien E, Kamil S, Rashid IU, Nadeem I (2021) Projected changes in climate extremes using CMIP6 simulations over SREX regions. Earth Syst Environ. https://doi.org/10.1007/s41748-021-00250-5

Chylek P, Li J, Dubey MK, Wang M, Lesins G (2011) Observed and model simulated 20th century Arctic temperature variability: Canadian Earth System Model CanESM2. Atmos Chem Phys Discuss 11:22893–22907. https://doi.org/10.5194/acpd-11-22893-2011

Collier MA, Jeffrey SJ, Rotstayn LD, Wong KKH, Dravitzki SM, Moeseneder C, Hamalainen C, Syktus JI, Suppiah R, Antony J, El Zein A, Atif M (2011) The CSIRO-Mk3.6.0 atmosphere-ocean GCM: participation in CMIP5 and data publication. In: Chan F, Marinova D, Anderssen R (eds) 19th international congress on modelling and simulation (MODSIM2011), CSIRO; Australian Govt, Bur Meteorol; Per Convent & Exhibit Ctr; Perth Convent Bur; Curtin Univ; Australian Math Soc (Aust MS); Australian & New Zealand Ind & Appl Math (ANZIAM); Australian Math Sci Inst (AMSI); Maralte Publishers; Econ Soc Australian (ES, pp 2691–2697)

Collins W, Bellouin N, Doutriaux-Boucher M, Gedney N, Hinton T, Jones CD, Liddicoat S, Martin G, O'Connor F, Rae J, Senior C, Totterdell I, Woodward S, Reichler T, Kim J (2008) Evaluation of HadGEM2 model. Meteorological Office Hadley Centre, Technical Note

Coumou D, Robinson A (2013) Historic and future increase in the global land area affected by monthly heat extremes. Environ Res Lett. https://doi.org/10.1088/1748-9326/8/3/034018

Cucchi M, Weedon GP, Amici A, Bellouin N, Lange S, Schmied HM, Hersbach H, Buontempo C (2020) WFDE5: bias-adjusted ERA5 reanalysis data for impact studies. Earth Syst Sci Data 12:2097–2120. https://doi.org/10.5194/essd-12-2097-2020

Dufresne JL, Foujols MA, Denvil S, Caubel A, Marti O, Aumont O, Balkanski Y, Bekki S, Bellenger H, Benshila R, Bony S, Bopp L, Braconnot P, Brockmann P, Cadule P, Cheruy F, Codron F, Cozic A, Cugnet D, de Noblet N, Duvel JP, Ethé C, Fairhead L, Fichefet T, Flavoni S, Friedlingstein P, Grandpeix JY, Guez L, Guilyardi E, Hauglustaine D, Hourdin F, Idelkadi A, Ghattas J, Joussaume S, Kageyama M, Krinner G, Labetoulle S, Lahellec A, Lefebvre MP, Lefevre F, Levy C, Li ZX, Lloyd J, Lott F, Madec G, Mancip M, Marchand M, Masson S, Meurdesoif Y, Mignot J, Musat I, Parouty S, Polcher J, Rio C, Schulz M, Swingedouw D, Szopa S, Talandier C, Terray P, Viovy N, Vuichard N (2013) Climate change projections using the IPSL-CM5 Earth System Model: from CMIP3 to CMIP5, vol 40. https://doi.org/10.1007/s00382-012-1636-1

Dunne JP, John JG, Adcroft AJ, Griffies SM, Hallberg RW, Shevliakova E, Stouffer RJ, Cooke W, Dunne KA, Harrison MJ, Krasting JP, Malyshev SL, Milly PC, Phillipps PJ, Sentman LT, Samuels BL, Spelman MJ, Winton M, Wittenberg AT, Zadeh N (2012) GFDL's ESM2 global coupled climate-carbon earth system models. Part I: physical formulation and baseline simulation characteristics. J Clim 25:6646–6665. https://doi.org/10.1175/JCLI-D-11-00560.1

El-Samra R, Bou-Zeid E, Bangalath HK, Stenchikov G, El-Fadel M (2018) Seasonal and regional patterns of future temperature extremes: high-resolution dynamic downscaling over a complex terrain. J Geophys Res Atmos 123:6669–6689. https://doi.org/10.1029/2017JD027500

Gent PR, Danabasoglu G, Donner LJ, Holland MM, Hunke EC, Jayne SR, Lawrence DM, Neale RB, Rasch PJ, Vertenstein M, Worley PH, Yang ZL, Zhang M (2011) The community climate system model version 4. J Clim 24:4973–4991. https://doi.org/10.1175/2011JCLI4083.1

Giorgetta MA, Jungclaus J, Reick CH, Legutke S, Bader J, Böttinger M, Brovkin V, Crueger T, Esch M, Fieg K, Glushak K, Gayler V, Haak H, Hollweg HD, Ilyina T, Kinne S, Kornblueh L, Matei D, Mauritsen T, Mikolajewicz U, Mueller W, Notz D, Pithan F, Raddatz T, Rast S, Redler R, Roeckner E, Schmidt H, Schnur R, Segschneider J, Six KD, Stockhause M, Timmreck C, Wegner J, Widmann H, Wieners KH, Claussen M, Marotzke J, Stevens B (2013) Climate and carbon cycle changes from 1850 to 2100 in MPI-ESM simulations for the Coupled Model Intercomparison Project phase 5. J Adv Model Earth Syst 5:572–597. https://doi.org/10.1002/jame.20038

Gosling SN, Lowe JA, McGregor GR, Pelling M, Malamud BD (2009) Associations between elevated atmospheric temperature and human mortality: a critical review of the literature. Clim Change 92(3–4):299–341. https://doi.org/10.1007/s10584-008-9441-x

Griffies SM, Winton M, Donner LJ, Horowitz LW, Downes SM, Farneti R, Gnanadesikan A, Hurlin WJ, Lee HC, Liang Z, Palter JB, Samuels BL, Wittenberg AT, Wyman BL, Yin J, Zadeh N (2011) The GFDL CM3 coupled climate model: characteristics of the ocean and sea ice simulations. J Clim 24:3520–3544. https://doi.org/10.1175/2011JCLI3964.1

IPCC (2013b) Annex i: Atlas of global and regional climate projections. In: van Oldenborgh GJ, Collins M et al (eds) In: Climate change 2013: the physical science basis. Contribution of working group I to the fifth assessment report of the intergovernmental panel on climate change [Stocker TF, Qin D, et al. (eds.)]. Cambridge University Press, Cambridge

Ji D, Wang L, Feng J, Wu Q, Cheng H, Zhang Q, Yang J, Dong W, Dai Y, Gong D, Zhang RH, Wang X, Liu J, Moore JC, Chen D, Zhou M (2014) Description and basic evaluation of Beijing Normal University Earth System Model (BNU-ESM) version 1. Geosci Model Dev 7:2039–2064. https://doi.org/10.5194/gmd-7-2039-2014

Karl TR, Knight RW, Easterling DR, Quayle RG (1996) Indices of climate change for the United States. Bull Am Meteorol Soc 77:279–292. https://doi.org/10.1175/1520-0477(1996)077<0279:IOCCFT>2.0.CO;2

Knutti R, Sedláček J (2013) Robustness and uncertainties in the new CMIP5 climate model projections. Nat Clim Change 3(4):369–373. https://doi.org/10.1038/nclimate1716

Legasa MN, Manzanas R, Fernández J, Herrera S, Iturbide M, Moufouma-Okia W, Zhai P, Driouech F, Gutiérrez JM (2020) Assessing multidomain overlaps and grand ensemble generation in CORDEX regional projections. Geophys Res Lett. https://doi.org/10.1029/2019GL086799

Lelieveld J, Hadjinicolaou P, Kostopoulou E, Chenoweth J, Maayar ME, Giannakopoulos C, Hannides C, Lange MA, Tanarhte M, Tyrlis E, Xoplaki E (2012) Climate change and impacts in the Eastern Mediterranean and the Middle East. Clim Change 114:667–687. https://doi.org/10.1007/s10584-012-0418-4

Lelieveld J, Proestos Y, Hadjinicolaou P, Tanarhte M, Tyrlis E, Zittis G (2016) Strongly increasing heat extremes in the Middle East and North Africa (MENA) in the 21st century. Clim Change 137:245–260. https://doi.org/10.1007/s10584-016-1665-6

Matthews T (2020) Death valley: world-beating temperatures, no sweat. Weather 75:347–348. https://doi.org/10.1002/wea.3858

Merlone A, Al-Dashti H, Faisal N, Cerveny RS, AlSarmi S, Bessemoulin P, Brunet M, Driouech F, Khalatyan Y, Peterson TC, Rahimzadeh F, Trewin B, Wahab MM, Yagan S, Coppa G, Smorgon D, Musacchio C, Krahenbuhl D (2019) Temperature extreme records: World Meteorological Organization metrological and meteorological evaluation of the 54.0°C observations in Mitribah, Kuwait and Turbat, Pakistan in 2016/2017. Int J Climatol 39:5154–5169. https://doi.org/10.1002/joc.6132

Mistry MN (2020) A high spatiotemporal resolution global gridded dataset of historical human discomfort indices. Atmosphere. https://doi.org/10.3390/ATMOS11080835

Mitchell D, Heaviside C, Vardoulakis S, Huntingford C, Masato G, Guillod BP, Frumhoff P, Bowery A, Wallom D, Allen M (2016) Attributing human mortality during extreme heat waves to anthropogenic climate change. Environ Res Lett. https://doi.org/10.1088/1748-9326/11/7/074006

Morak S, Hegerl GC, Kenyon J (2011) Detectable regional changes in the number of warm nights. Geophys Res Lett. https://doi.org/10.1029/2011GL048531

Mueller B, Seneviratne SI (2012) Hot days induced by precipitation deficits at the global scale. Proc Natl Acad Sci USA 109:12398–12403. https://doi.org/10.1073/pnas.1204330109

Mueller B, Zhang X, Zwiers FW (2016) Historically hottest summers projected to be the norm for more than half of the world's population within 20 years. Environ Res Lett. https://doi.org/10.1088/1748-9326/11/4/044011

Ntoumos A, Hadjinicolaou P, Zittis G, Lelieveld J (2020) Updated assessment of temperature extremes over the Middle East-North Africa (MENA) region from observational and CMIP5 data. Atmosphere. https://doi.org/10.3390/ATMOS11080813

Ozturk T, Saygili-Araci FS, Kurnaz ML (2021) Projected changes in extreme temperature and precipitation indices over CORDEX-MENA domain. Atmosphere. https://doi.org/10.3390/atmos12050622

Pal JS, Eltahir EA (2016) Future temperature in southwest Asia projected to exceed a threshold for human adaptability. Nat Clim Change 6:197–200. https://doi.org/10.1038/nclimate2833

Perkins-Kirkpatrick SE, Lewis SC (2020) Increasing trends in regional heatwaves. Nat Commun. https://doi.org/10.1038/s41467-020-16970-7

Rothfus LP (1990) The heat index equation. National Weather Service Technical Attachment p SR, Fort Worth, TX, pp 90–23

Russo A, Gouveia CM, Dutra E, Soares PM, Trigo RM (2019) The synergy between drought and extremely hot summers in the Mediterranean. Environ Res Lett. https://doi.org/10.1088/1748-9326/aaf09e

Russo S, Sillmann J, Sterl A (2017) Humid heat waves at different warming levels. Sci Rep. https://doi.org/10.1038/s41598-017-07536-7

Schwingshackl C, Sillmann J, Vicedo-Cabrera AM, Sandstad M, Aunan K (2021) Heat stress indicators in cmip6: estimating future trends and exceedances of impact-relevant thresholds. Earth's Future. https://doi.org/10.1029/2020EF001885

Seneviratne SI, Donat MG, Pitman AJ, Knutti R, Wilby RL (2016) Allowable CO2 emissions based on regional and impact-related climate targets. Nature 529:477–483. https://doi.org/10.1038/nature16542

Sillmann J, Kharin VV, Zhang X, Zwiers FW, Bronaugh D (2013) Climate extremes indices in the CMIP5 multimodel ensemble: Part 1. Model evaluation in the present climate. J Geophys Res Atmos 118:1716–1733. https://doi.org/10.1002/jgrd.50203

Sillmann J, Kharin VV, Zwiers FW, Zhang X, Bronaugh D (2013) Climate extremes indices in the CMIP5 multimodel ensemble: Part 2. Future climate projections. J Geophys Res Atmos 118:2473–2493. https://doi.org/10.1002/jgrd.50188

Steadman R (1979) The assessment of sultriness. Part I: a temperature-humidity index based on human physiology and clothing science. J Appl Meteorol Climatol 7:861–873. https://doi.org/10.1175/1520-0450(1979)018<0861:TAOSPI>2.0.CO;2

Tanarhte M, Hadjinicolaou P, Lelieveld J (2012) Intercomparison of temperature and precipitation data sets based on observations in the Mediterranean and the Middle East. J Geophys Res Atmos. https://doi.org/10.1029/2011JD017293

Tank AMK, Zwiers FW, Zhang X (2009) WMO guidelines on extremes guidelines on analysis of extremes in a changing climate in support of informed decisions. Climate data and monitoring, p 52, file attachment

Taylor KE, Stouffer RJ, Meehl GA (2012) An overview of CMIP5 and the experiment design. Bull Am Meteorol Soc 93:485–498. https://doi.org/10.1175/BAMS-D-11-00094.1

...Tongwen WU, Lianchun S, Weiping L, Zaizhi W, Hua Z, Xiaoge X, Yanwu Z, Li Z, Jianglong L, Fanghua W, Yiming L, Fang Z, Xueli S, Min CHU, Jie Z, Yongjie F, Fang W, Yixiong L, Xiangwen L, Min W, Qianxia L, Wenyan Z, Min D, Qiqeng Z, Jinjun J, Li L, Mingyu Z (2014) An overview of BCC climate system model development. J Meteorol Res 28:34–56. https://doi.org/10.1007/s13351-014-3041-7.Supported

Vogel MM, Hauser M, Seneviratne SI (2020) Projected changes in hot, dry and wet extreme events' clusters in CMIP6 multi-model ensemble. Environ Res Lett. https://doi.org/10.1088/1748-9326/ab90a7

Voldoire A, Sanchez-Gomez E, y Mélia DS, Decharme B, Cassou C, Sénési S, Valcke S, Beau I, Alias A, Chevallier M, Déqué M, Deshayes J, Douville H, Fernandez E, Madec G, Maisonnave E, Moine MP, Planton S, Saint-Martin D, Szopa S, Tyteca S, Alkama R, Belamari S, Braun A, Coquart L, Chauvin F, (2013) The CNRM-CM5.1 global climate model: description and basic evaluation. Clim Dyn 40:2091–2121. https://doi.org/10.1007/s00382-011-1259-y

Vuuren DPV, Edmonds J, Kainuma M, Riahi K, Thomson A, Hibbard K, Hurtt GC, Kram T, Krey V, Lamarque JF, Masui T, Meinshausen M, Nakicenovic N, Smith SJ, Rose SK (2011) The representative concentration pathways: an overview. Clim Change 109:5–31. https://doi.org/10.1007/s10584-011-0148-z

Waha K, Krummenauer L, Adams S, Aich V, Baarsch F, Coumou D, Fader M, Hoff H, Jobbins G, Marcus R, Mengel M, Otto IM, Perrette M, Rocha M, Robinson A, Schleussner CF (2017) Climate change impacts in the middle east and Northern Africa (Mena) region and their implications for vulnerable population groups. Reg Environ Change 17:1623–1638. https://doi.org/10.1007/s10113-017-1144-2

Watanabe M, Suzuki T, O'Ishi R, Komuro Y, Watanabe S, Emori S, Takemura T, Chikira M, Ogura T, Sekiguchi M, Takata K, Yamazaki D, Yokohata T, Nozawa T, Hasumi H, Tatebe H, Kimoto M (2010) Improved climate simulation by MIROC5: mean states, variability, and climate sensitivity. J Clim 23:6312–6335. https://doi.org/10.1175/2010JCLI3679.1

Watanabe S, Hajima T, Sudo K, Nagashima T, Takemura T, Okajima H, Nozawa T, Kawase H, Abe M, Yokohata T, Ise T, Sato H, Kato E, Takata K, Emori S, Kawamiya M (2011) MIROC-ESM 2010: model description and basic results of CMIP5-20c3m experiments. Geosci Model Dev 4:845–872. https://doi.org/10.5194/gmd-4-845-2011

Yukimoto S, Adachi Y, Hosaka M, Sakami T, Yoshimura H, Hirabara M, Tanaka TY, Shindo E, Tsujino H, Deushi M, Mizuta R, Yabu S, Obata A, Nakano H, Koshiro T, Ose T, Kitoh A (2012) A new global climate model of the Meteorological Research Institute: MRI-CGCM3: model description and basic performance-. J Meteorol Soc Jpn 90:23–64. https://doi.org/10.2151/jmsj.2012-A02

Zhang X, Alexander L, Hegerl GC, Jones P, Tank AK, Peterson TC, Trewin B, Zwiers FW (2011) Indices for monitoring changes in extremes based on daily temperature and precipitation data. Wiley Interdiscip Rev Clim Change 2:851–870. https://doi.org/10.1002/wcc.147

Zittis G (2018) Observed rainfall trends and precipitation uncertainty in the vicinity of the Mediterranean, Middle East and North Africa. Theor Appl Climatol 134:1207–1230. https://doi.org/10.1007/s00704-017-2333-0

Zittis G, Hadjinicolaou P, Lelieveld J (2014) Role of soil moisture in the amplification of climate warming in the eastern Mediterranean and the Middle East. Clim Res 59:27–37. https://doi.org/10.3354/cr01205

Zittis G, Hadjinicolaou P, Lelieveld J, Fnais M (2016) Projected changes in heat wave characteristics in the Eastern Mediterranean and the Middle East. Reg Environ Change 1863—1876

Zittis G, Hadjinicolaou P, Almazroui M, Bucchignani E, Driouech F, Rhaz KE, Kurnaz L, Nikulin G, Ntoumos A, Ozturk T, Proestos

Y, Stenchikov G, Zaaboul R, Lelieveld J (2021) Business-as-usual will lead to super and ultra-extreme heatwaves in the Middle East and North Africa. NPJ Clim Atmos Sci. https://doi.org/10.1038/s41612-021-00178-7